



ELSEVIER

Physics Letters B 541 (2002) 45–51

PHYSICS LETTERS B

[www.elsevier.com/locate/npe](http://www.elsevier.com/locate/npe)

# Measurement of $\Gamma(\phi \rightarrow \eta'\gamma)/\Gamma(\phi \rightarrow \eta\gamma)$ and the pseudoscalar mixing angle

KLOE Collaboration

A. Aloisio<sup>f</sup>, F. Ambrosino<sup>f,\*</sup>, A. Antonelli<sup>c</sup>, M. Antonelli<sup>c</sup>, C. Bacci<sup>j</sup>, G. Bencivenni<sup>c</sup>, S. Bertolucci<sup>c</sup>, C. Bini<sup>h</sup>, C. Bloise<sup>c</sup>, V. Bocci<sup>h</sup>, F. Bossi<sup>c</sup>, P. Branchini<sup>j</sup>, S.A. Bulychjov<sup>o</sup>, G. Cabibbo<sup>h</sup>, R. Caloi<sup>h</sup>, P. Campana<sup>c</sup>, G. Capon<sup>c</sup>, G. Carboni<sup>i</sup>, M. Casarsa<sup>m</sup>, V. Casavola<sup>e</sup>, G. Cataldi<sup>e</sup>, F. Ceradini<sup>j</sup>, F. Cervelli<sup>k</sup>, F. Cevenini<sup>f</sup>, G. Chiefari<sup>f</sup>, P. Ciambrone<sup>c</sup>, S. Conetti<sup>b</sup>, E. De Lucia<sup>h</sup>, G. De Robertis<sup>a</sup>, P. De Simone<sup>c</sup>, G. De Zorzi<sup>h</sup>, S. Dell'Agello<sup>c</sup>, A. Denig<sup>c</sup>, A. Di Domenico<sup>h</sup>, C. Di Donato<sup>f</sup>, S. Di Falco<sup>k</sup>, A. Doria<sup>f</sup>, M. Dreucci<sup>c</sup>, O. Erriquez<sup>a</sup>, A. Farilla<sup>j</sup>, G. Felici<sup>c</sup>, A. Ferrari<sup>j</sup>, M.L. Ferrer<sup>c</sup>, G. Finocchiaro<sup>c</sup>, C. Forti<sup>c</sup>, A. Franceschi<sup>c</sup>, P. Franzini<sup>h</sup>, C. Gatti<sup>k</sup>, P. Gauzzi<sup>h</sup>, S. Giovannella<sup>c</sup>, E. Gorini<sup>e</sup>, F. Grancagnolo<sup>e</sup>, E. Graziani<sup>j</sup>, S.W. Han<sup>c,n</sup>, M. Incagli<sup>k</sup>, L. Ingrosso<sup>c</sup>, W. Kluge<sup>d</sup>, C. Kuo<sup>d</sup>, V. Kulikov<sup>o</sup>, F. Lacava<sup>h</sup>, G. Lanfranchi<sup>c</sup>, J. Lee-Franzini<sup>c,l</sup>, D. Leone<sup>h</sup>, F. Lu<sup>c,n</sup>, M. Martemianov<sup>d</sup>, M. Matsyuk<sup>c,o</sup>, W. Mei<sup>c</sup>, L. Merola<sup>f</sup>, R. Messi<sup>i</sup>, S. Miscetti<sup>c</sup>, M. Moulson<sup>c</sup>, S. Müller<sup>d</sup>, F. Murtas<sup>c</sup>, M. Napolitano<sup>f</sup>, A. Nedosekin<sup>c,o</sup>, F. Nguyen<sup>j</sup>, M. Palutan<sup>j</sup>, L. Paoluzi<sup>i</sup>, E. Pasqualucci<sup>h</sup>, L. Passalacqua<sup>c</sup>, A. Passeri<sup>j</sup>, V. Patera<sup>c,g</sup>, E. Petrolo<sup>h</sup>, G. Pirozzi<sup>f</sup>, C. Pistillo<sup>f</sup>, L. Pontecorvo<sup>h</sup>, M. Primavera<sup>e</sup>, F. Ruggieri<sup>a</sup>, P. Santangelo<sup>c</sup>, E. Santovetti<sup>i</sup>, G. Saracino<sup>f</sup>, R.D. Schamberger<sup>l</sup>, B. Sciascia<sup>h</sup>, A. Sciubba<sup>c,g</sup>, F. Scuri<sup>m</sup>, I. Sfiligoi<sup>c</sup>, T. Spadaro<sup>h</sup>, E. Spiriti<sup>j</sup>, G.L. Tong<sup>c,n</sup>, L. Tortora<sup>j</sup>, E. Valente<sup>h</sup>, P. Valente<sup>c</sup>, B. Valeriani<sup>d</sup>, G. Venanzoni<sup>k</sup>, S. Veneziano<sup>h</sup>, A. Ventura<sup>e</sup>, Y. Xu<sup>c,n</sup>, Y. Yu<sup>c,n</sup>

<sup>a</sup> Dipartimento di Fisica dell'Università e Sezione INFN, Bari, Italy

<sup>b</sup> Physics Department, University of Virginia, VA, USA

<sup>c</sup> Laboratori Nazionali di Frascati dell'INFN, Frascati, Italy

<sup>d</sup> Institut für Experimentelle Kernphysik, Universität Karlsruhe, Germany

<sup>e</sup> Dipartimento di Fisica dell'Università e Sezione INFN, Lecce, Italy

<sup>f</sup> Dipartimento di Scienze Fisiche dell'Università "Federico II" e Sezione INFN, Napoli, Italy

<sup>g</sup> Dipartimento di Energetica dell'Università "La Sapienza", Roma, Italy

<sup>h</sup> Dipartimento di Fisica dell'Università "La Sapienza" e Sezione INFN, Roma, Italy

<sup>i</sup> Dipartimento di Fisica dell'Università "Tor Vergata" e Sezione INFN, Roma, Italy

<sup>j</sup> Dipartimento di Fisica dell'Università "Roma Tre" e Sezione INFN, Roma, Italy

<sup>k</sup> Dipartimento di Fisica dell'Università e Sezione INFN, Pisa, Italy

<sup>l</sup> Physics Department, State University of New York at Stony Brook, USA

<sup>m</sup> Dipartimento di Fisica dell'Università e Sezione INFN, Trieste, Italy

<sup>n</sup> Permanent address: Institute of High Energy Physics, CAS, Beijing, China

<sup>o</sup> Permanent address: Institute for Theoretical and Experimental Physics, Moscow, Russia

Received 8 June 2002; accepted 17 June 2002

Editor: L. Montanet

---

## Abstract

We have measured the radiative decays  $\phi \rightarrow \eta\gamma$ ,  $\phi \rightarrow \eta'\gamma$  selecting  $\pi^+\pi^-\gamma\gamma\gamma$  final state in a sample of  $\sim 5 \times 10^7$   $\phi$ -mesons produced at the Frascati  $\phi$ -factory DAΦNE. We obtain  $\Gamma(\phi \rightarrow \eta'\gamma)/\Gamma(\phi \rightarrow \eta\gamma) = (4.70 \pm 0.47 \pm 0.31) \times 10^{-3}$ . From this result we derive new accurate values for the branching ratio  $\text{BR}(\phi \rightarrow \eta'\gamma) = (6.10 \pm 0.61 \pm 0.43) \times 10^{-5}$  and the mixing angle of pseudoscalar mesons in the flavour basis  $\varphi_P = (41.8_{-1.6}^{+1.9})^\circ$ . © 2002 Elsevier Science B.V. All rights reserved.

PACS: 13.65.+i; 14.40.Aq

Keywords:  $e^+e^-$  collisions;  $\phi$  radiative decays; Pseudoscalar mixing angle

---

Radiative decays of light vector mesons to pseudoscalars have been a source of precious information since the early days of the quark model [1]. They have been studied in the context of chiral Lagrangians by several authors [2]. The branching ratio (BR) of the decay  $\phi \rightarrow \eta'\gamma$  is particularly interesting since its value can probe the  $s\bar{s}$  and gluonium contents of the  $\eta'$  [3] or the amount of nonet symmetry breaking [4]. In particular, the ratio  $R = \text{BR}(\phi \rightarrow \eta'\gamma)/\text{BR}(\phi \rightarrow \eta\gamma)$  can be related to the  $\eta$ - $\eta'$  mixing parameters [5–9] and determines the pseudoscalar mixing angle. Even for the case of two mixing angles which appears in extended chiral perturbation theory [10], as well as from phenomenological analyses [11], it has been argued that the two mixing parameters in the flavour basis are equal apart from terms which violate the Okubo–Zweig–Iizuka (OZI) rule [12,13]. It is thus possible to parameterize mixing in a nearly process independent way by just one mixing angle,  $\varphi_P$ . The large  $\text{BR}(B \rightarrow K\eta')$  value observed [14], as opposed to theoretical predictions [15], raises also interest [16] about the gluonium contents of the  $\eta'$ . This can also be tested from a precise determination of  $\text{BR}(\phi \rightarrow \eta'\gamma)$ . The  $\text{BR}(\phi \rightarrow \eta'\gamma)$  measurements available to date still have rather large uncertainties [17–19]. The study of  $\phi \rightarrow \eta'\gamma$  decays presented in the following,

is based on an integrated luminosity of  $\sim 16 \text{ pb}^{-1}$  corresponding to some  $5 \times 10^7$   $\phi$  decays collected by the KLOE detector [20] at DAΦNE [21], the Frascati  $e^+e^-$  collider, during the year 2000. All data were taken at a total energy  $w = M_\phi$ .

The KLOE detector consists of a large cylindrical drift chamber (DC), surrounded by a lead-scintillating fibers electromagnetic calorimeter (EmC). A superconducting coil surrounds the EmC and provides a 0.52 T field along the beam axis. The DC [22], 4 m diameter and 3.3 m long, has 12 582 all-stereo tungsten sense wires and 37 746 aluminum field wires. The chamber shell is made of carbon fiber-epoxy composite and the gas used is a 90% helium, 10% isobutane mixture. These choices maximize transparency to photons and reduce  $K_L \rightarrow K_S$  regeneration as well as multiple scattering. Momentum resolution is  $\sigma(p_\perp)/p_\perp \sim 0.4\%$ . Position resolution is  $\sigma_{xy} \sim 150 \mu\text{m}$  and  $\sigma_z \sim 2 \text{ mm}$ . Vertices are reconstructed with an accuracy of  $\sim 3 \text{ mm}$ . The EmC [23] is divided into a barrel and two end-caps, for a total of 88 modules, and covers 98% of the solid angle. The modules are read out at both ends by photomultipliers. Readout granularity is  $\sim 4.4 \times 4.4 \text{ cm}^2$ , for a total of 2 440 “cells”. Arrival times and positions in three dimensions of energy deposits are determined from the signals at the two ends. Cells close in time and space are grouped into a calorimeter cluster. The cluster energy  $E_{\text{CL}}$  is the sum of the cell energies.

---

\* Corresponding author.

E-mail address: fabio.ambrosino@na.infn.it (F. Ambrosino).

Cluster time  $t_{\text{CL}}$  and position  $\vec{r}_{\text{CL}}$ , are energy weighed averages. Resolutions are  $\sigma_E/E = 5.7\%/\sqrt{E(\text{GeV})}$  and  $\sigma_t = 57 \text{ ps}/\sqrt{E(\text{GeV})} \oplus 50 \text{ ps}$ . The detector trigger [24] uses calorimeter and chamber information.

To determine  $R$  we search for events [25]:

- (1)  $\phi \rightarrow \eta'\gamma$ ; with  $\eta' \rightarrow \pi^+\pi^-\eta$  and  $\eta \rightarrow \gamma\gamma$ ,
- (2)  $\phi \rightarrow \eta\gamma$ ; with  $\eta \rightarrow \pi^+\pi^-\pi^0$  and  $\pi^0 \rightarrow \gamma\gamma$ .

The final state is  $\pi^+\pi^-\gamma\gamma\gamma$  for both reactions. Most systematics uncertainties therefore approximately cancel in measuring  $R$ .  $\phi \rightarrow \eta\gamma$  decays are easily selected with small background and provide a clean control sample for the analysis. Process (2), about 100 times more abundant than (1), is the main source of background for  $\phi \rightarrow \eta'\gamma$  events. Further background is due to:

- (3)  $\phi \rightarrow K_S K_L$  events with one charged vertex where at least one photon is not detected and the  $K_L$  is decaying near the interaction region (IR),
- (4)  $\phi \rightarrow \pi^+\pi^-\pi^0$  events with an additional photon detected due to accidental clusters or splitting of clusters in the EmC.

After some trivial cuts to remove radiative Bhabhas and machine background events, we select events satisfying the following cuts:

- (a) Exactly three photons with  $21^\circ < \theta_\gamma < 159^\circ$  and  $E_\gamma > 10 \text{ MeV}$ .
- (b) Opening angle of each photon pair  $> 18^\circ$ .
- (c) A vertex inside the cylindrical region  $\sqrt{x^2 + y^2} < 4 \text{ cm}$ ;  $|z| < 8 \text{ cm}$  with two opposite charge tracks.

A photon candidate is a calorimeter cluster with no track pointing to it and  $|(t_{\text{CL}} - |\vec{r}_{\text{CL}}|/c)| < 5\sigma_t(E_{\text{CL}})$ . Small angles are excluded to reduce machine background. The opening angle cut ensures that fragments of clusters are not counted as separate photons. At this level the ratio of the two efficiencies is  $\epsilon_{\eta'\gamma}/\epsilon_{\eta\gamma} = 0.9$ . It is close to one, given the similarities among the two processes. The residual difference is due to the efficiency in tracking the pions to the origin, because of their different momentum spectra for the two processes. After this first level selection we perform a kinematic fit requiring energy–momentum conserva-

tion and photon candidates times and path lengths to be consistent with the speed of light. Particle masses are not constrained. We require  $\text{prob}(\chi^2) > 1\%$  for both processes (1) and (2).

The only additional cuts applied to select process (2) are a very loose cut on the energy of the radiative photon (after kinematic fit) and a cut on pion energy endpoint. The radiative photon can be easily identified being the hardest in the event for process (2). We require:

- (d)  $320 \text{ MeV} < E_\gamma^{\text{rad.}} < 400 \text{ MeV}$ .
- (e)  $E_{\pi^+} + E_{\pi^-} < 550 \text{ MeV}$ .

The first cut is very effective in reducing residual background from process (3) where the endpoint for photon energies is at 280 MeV. The second cut eliminates residual background from process (4). Both cuts have full efficiency for the signal. We are then left with  $N_{\eta\gamma} = 50210 \pm 220$  events. The overall efficiency for detecting  $\phi \rightarrow \eta\gamma$  events is evaluated from Monte Carlo simulations (MC) to be 36.5%. Background is expected to be below 0.5%, and all observed distributions are in agreement with this estimate. The abundant and pure  $\phi \rightarrow \eta\gamma$  events are used as a control sample to evaluate systematic effects on the efficiencies by comparing data and MC distributions for the variable to which cuts are applied. The distributions exhibit a remarkable agreement, as shown in Fig. 1 for the photons energy spectrum.

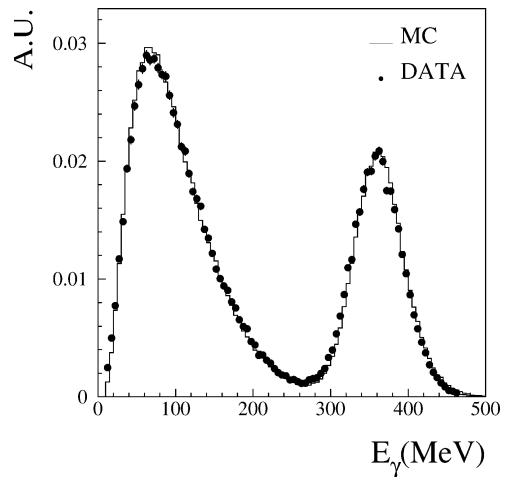


Fig. 1. Data: MC comparison for the energy spectrum of photons in events selected as  $\phi \rightarrow \eta\gamma \rightarrow \pi^+\pi^-\gamma\gamma$ .

Process (1) events require, in addition to (a)–(c):

- (f)  $E_{\pi^+} + E_{\pi^-} < 430$  MeV.
- (g)  $\Sigma_{\gamma} E_{\gamma} > 540$  MeV.

These cuts are quite effective in suppressing events from process (3) and (4), respectively. We estimate a residual background of less than 18 events from reactions 3 and 4. Contamination from process (2) is however still high. About 35% of  $\phi \rightarrow \eta\gamma$  events are still in the  $\phi \rightarrow \eta'\gamma$  sample for a S/B ratio of  $\sim 5 \times 10^{-3}$ . To separate  $\eta'\gamma$  and  $\eta\gamma$  events we use the correlation between the energies  $E_1$  and  $E_2$  of the two most energetic photons in the event. Event densities in

the  $E_1$ – $E_2$  plane are shown in Fig. 2; for  $\eta'\gamma$  events they are strongly anticorrelated (see MC distribution, Fig. 2(a)) while for  $\eta\gamma$  events they are concentrated in two narrow bands around  $E_1$  or  $E_2 = 363$  MeV which is the energy of the radiative photon (see MC events in Fig. 2(b)). We select  $\eta'\gamma$  candidate events inside the elliptical shaped region as shown in Fig. 2(c) for the experimental data. The  $\pi^+\pi^-\gamma\gamma$  invariant mass for the events inside the selection ellipse is plotted in Fig. 3. We notice a clear peak at the  $\eta'$  mass value with the width expected from MC, over a small residual background. The  $\eta'\gamma$  signal is obtained by a fit in the region  $942 \leq M_{\pi^+\pi^-\gamma\gamma} \leq 974$  MeV. For the signal we use the MC shape. The background

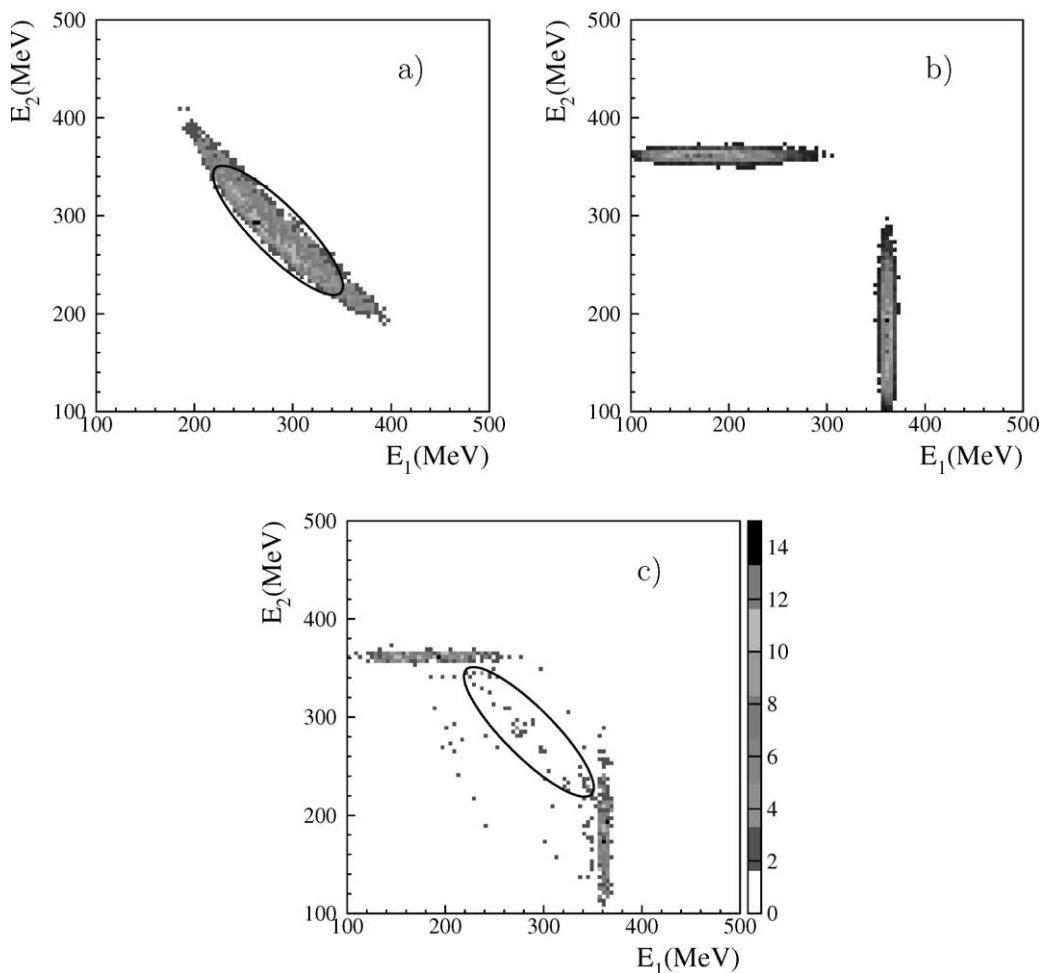


Fig. 2. Event density distributions in the  $E_1$ – $E_2$  plane. (a) MC for  $\eta'\gamma$  events; (b) MC for  $\eta\gamma$  events; (c) Experimental data after first level selection; events in the  $\eta\gamma$  bands have been downscaled for clarity. The number of observed events inside the ellipse is 175.

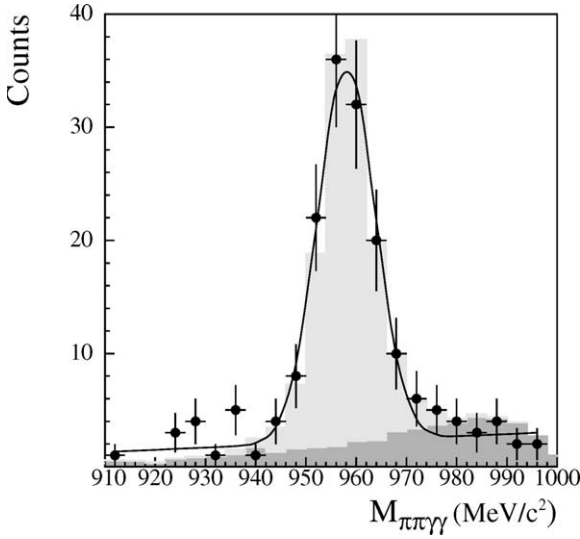


Fig. 3. The  $\pi^+\pi^-\gamma\gamma$  invariant mass for events selected as  $\phi \rightarrow \eta'\gamma$  candidates. The shaded areas represent signal (shape from MC) and background (shape from sidebands analysis of data). The continuous line is the result of a Gaussian plus linear fit.

shape is derived from sidebands selected in the  $E_1$ – $E_2$  plane just outside the acceptance ellipse. The final number of events from process (1), after background subtraction, is  $N_{\eta'\gamma} = 120 \pm 12(\text{stat.}) \pm 5(\text{syst.})$ . The overall efficiency for  $\eta'\gamma$  events is  $\epsilon_{\eta'\gamma} = 22.8\%$ .

The ratio of the branching ratios  $R = \text{BR}(\phi \rightarrow \eta'\gamma)/\text{BR}(\phi \rightarrow \eta\gamma)$  is determined from:

$$R = \frac{N_{\eta'\gamma}}{N_{\eta\gamma}} \left( \frac{\epsilon_{\eta\gamma}}{\epsilon_{\eta'\gamma}} \right) \times \frac{\text{BR}(\eta \rightarrow \pi^+\pi^-\pi^0)\text{BR}(\pi^0 \rightarrow \gamma\gamma)}{\text{BR}(\eta' \rightarrow \pi^+\pi^-\eta)\text{BR}(\eta \rightarrow \gamma\gamma)} K_\rho.$$

$K_\rho = 0.95$  is a correction factor to the observed cross sections due to the interference between the amplitudes  $A(\phi \rightarrow \eta(\eta')\gamma)$  and  $A(\rho \rightarrow \eta(\eta')\gamma)$  at  $\sqrt{s} = m_\phi$ . The correction factor  $K_\rho$  has been evaluated [25], in a way similar to [26], using the Gounaris–Sakurai [27] parameterization of the  $\rho$  and accounting for the quark model phases which imply positive interference for  $\eta'\gamma$  and negative interference for  $\eta\gamma$  final state. Using the values in Table 1 we get

$$R = (4.70 \pm 0.47(\text{stat.}) \pm 0.31(\text{syst.})) \times 10^{-3}.$$

Systematics on luminosity and  $\phi$  cross section cancel out in the ratio exactly. Other effects, such as trig-

ger and reconstruction efficiencies, and machine background accidentals also partially cancel out in evaluating  $R$ . The systematic error is thus dominated by the uncertainties on background subtraction and on the intermediate branching fractions [17].

Using the current PDG [17] value for  $\text{BR}(\phi \rightarrow \eta\gamma)$  we extract the most precise determination of  $\text{BR}(\phi \rightarrow \eta'\gamma)$  to date:

$$\begin{aligned} \text{BR}(\phi \rightarrow \eta'\gamma) \\ = 6.10 \pm 0.61(\text{stat.}) \pm 0.43(\text{syst.}) \times 10^{-5}. \end{aligned}$$

The value we obtain for  $R$  can be related directly to the mixing angle in the flavour basis. In the approach by Bramon et al. [7], where SU(3) breaking is taken into account via a constituent quark mass ratio  $m_s/\bar{m}$ , one has:

$$R = \cot^2 \varphi_P \left( 1 - \frac{m_s \tan \varphi_V}{\bar{m} \sin 2\varphi_P} \right)^2 \left( \frac{p_{\eta'}}{p_\eta} \right)^3, \quad (1)$$

where  $\varphi_V = 3.4^\circ$  is the deviation from ideal mixing for vector mesons and  $p_{\eta(\eta')}$  is the radiative photon momentum in the  $\phi$  center of mass. Feldmann [9] (following [6]) combines chiral anomaly predictions for  $P \rightarrow \gamma\gamma$  with vector dominance to extract the couplings  $g_{\phi\eta\gamma}$  and  $g_{\phi\eta'\gamma}$ . Then, apart from OZI rule violating terms:

$$R = \left( \frac{\sin \varphi_P \sin \varphi_V}{6f_q} - \frac{\cos \varphi_P}{3f_s} \right)^2 \left/ \left( \frac{\cos \varphi_P \sin \varphi_V}{6f_q} + \frac{\sin \varphi_P}{3f_s} \right)^2 \right. \left( \frac{p_{\eta'}}{p_\eta} \right)^3, \quad (2)$$

where  $f_q$  and  $f_s$  are the pseudoscalar decay constants in the flavour basis. Values for all the parameters (except  $\varphi_P$ ) in Eqs. (1) and (2) are from the quoted papers. Both approaches give very similar results:

$$\varphi_{P-(1)} = (41.8_{-1.6}^{+1.9})^\circ \quad \text{and}$$

$$\varphi_{P-(2)} = (42.2 \pm 1.7)^\circ,$$

respectively. An estimate of the uncertainty on the extraction of  $\varphi_P$  using these approaches is  $\mathcal{O}(0.5^\circ)$ . This is suggested by the difference among the two values above and reflects the spread of the  $m_s/\bar{m}$ ,  $f_s$  and  $f_q$  values found in the literature. The  $\varphi_P$  value above is equivalent to a mixing angle of  $\theta_P = (-12.9_{-1.6}^{+1.9})^\circ$  in the octet-singlet basis. The mixing angle value has been obtained neglecting OZI rule

Table 1

Contributions to the systematic error on  $R$ . The systematics evaluation on the ratio of analysis efficiencies is obtained from the study of the  $\eta\gamma$  sample and varying the selection cuts. The intermediate BR's and errors are taken from [17]

Quantity	Value	Systematic error
$N_{\eta'\gamma}/N_{\eta\gamma}$	$2.39 \times 10^{-3}$	4.2% (background)
$\frac{\epsilon_{\eta\gamma}}{\epsilon_{\eta'\gamma}}$	1.60	Preselection 2.2% Photon counting 0.8% Vertex efficiency 0.9% Prob( $\chi^2$ ) 2.3% Accidentals 0.5%
$\frac{\text{BR}(\eta \rightarrow \pi^+ \pi^- \pi^0) \text{BR}(\pi^0 \rightarrow \gamma\gamma)}{\text{BR}(\eta' \rightarrow \pi^+ \pi^- \eta) \text{BR}(\eta \rightarrow \gamma\gamma)}$	1.30	3.8%
Total		6.6%

violation and a possible gluonium contents of the  $\eta$  and  $\eta'$  mesons. Allowing for gluonium [5] we write:

$$|\eta\rangle = X_\eta |u\bar{u} + d\bar{d}\rangle / \sqrt{2} + Y_\eta |s\bar{s}\rangle + Z_\eta |\text{glue}\rangle,$$

$$|\eta'\rangle = X_{\eta'} |u\bar{u} + d\bar{d}\rangle / \sqrt{2} + Y_{\eta'} |s\bar{s}\rangle + Z_{\eta'} |\text{glue}\rangle. \quad (3)$$

A gluonium component of the  $\eta'$  corresponds to  $Z_{\eta'}^2 > 0$  or equivalently  $X_{\eta'}^2 + Y_{\eta'}^2 < 1$ . Constraints on  $X_{\eta'}$  and  $Y_{\eta'}$  can be obtained in a nearly model-independent way by using the following relations:

$$\frac{\Gamma(\eta' \rightarrow \rho\gamma)}{\Gamma(\omega \rightarrow \pi^0\gamma)} \simeq 3 \left( \frac{m_{\eta'}^2 - m_\rho^2}{m_\omega^2 - m_\pi^2} \frac{m_\omega}{m_{\eta'}} \right)^3 X_{\eta'}^2 \quad (4)$$

and

$$\frac{\Gamma(\eta' \rightarrow \gamma\gamma)}{\Gamma(\pi^0 \rightarrow \gamma\gamma)} = \frac{1}{9} \left( \frac{m_{\eta'}}{m_{\pi^0}} \right)^3 \left( 5X_{\eta'} + \sqrt{2}Y_{\eta'} \frac{f_\pi}{f_s} \right)^2 \quad (5)$$

which are based on simple SU(3) ideas, exploiting the magnetic dipole nature of the transitions  $V \rightarrow P\gamma$  and  $P \rightarrow V\gamma$  by deriving the two photon couplings from the Wess–Zumino–Witten term of the chiral Lagrangian [5,8,16]. A consistency check of the assumption of  $\eta$ – $\eta'$  mixing without gluonium can be performed as follows: if  $Z_{\eta'} = 0$  one has  $|Y_{\eta'}| = \cos\varphi_P$ . This remains a reasonable approximation if the gluonium component is small. In Fig. 4 we plot in the  $X_{\eta'}$ ,  $Y_{\eta'}$  plane the allowed bands corresponding to relations (4), (5) and to our measurement of  $\cos\varphi_P$ , as well as the circumference  $X_{\eta'}^2 + Y_{\eta'}^2 = 1$ , corresponding to zero gluonium in the  $\eta'$ . We thus find  $Z_{\eta'}^2 = 0.06^{+0.09}_{-0.06}$ , compatible with zero within  $1\sigma$  and consistent with a gluonium fraction below 15%.

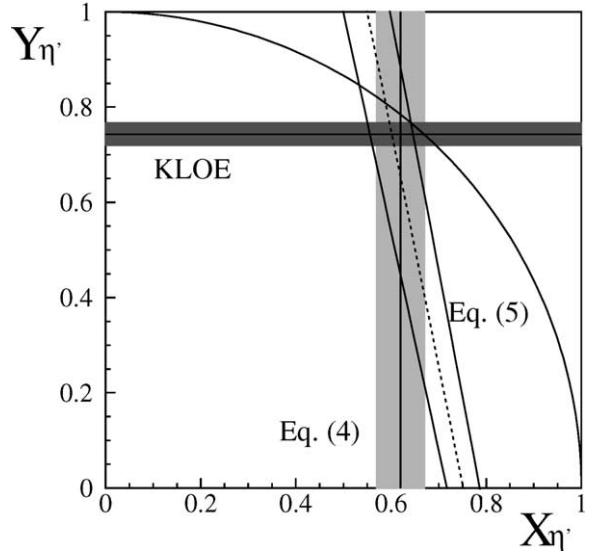


Fig. 4. Bounds on  $X_{\eta'}$  and  $Y_{\eta'}$  from SU(3) calculations and experimental branching fractions. The horizontal band is the KLOE result in the assumption  $Z_{\eta'} = 0$ .

## Acknowledgements

We thank the DAΦNE team for their efforts in maintaining low background running conditions and their collaboration during all data-taking. We also thank Giuseppe Fabio Fortugno for his efforts in ensuring good operations of the KLOE computing facilities. We thank R. Escribano and N. Paver for fruitful discussions. This work was supported in part by DOE grant DE-FG-02-97ER41027; by EURO-DAPHNE, contract FMRX-CT98-0169; by the German Federal Ministry of Education and Research

(BMBF) contract 06-KA-957; by Graduiertenkolleg ‘H.E. Phys. and Part. Astrophys.’ of Deutsche Forschungsgemeinschaft, Contract No. GK 742; by INTAS, contracts 96-624, 99-37; and by TARI, contract HPRI-CT-1999-00088.

## References

- [1] C. Becchi, G. Morpurgo Phys. Rev. 140 (1965) B687.
- [2] A. Bramon, A. Grau, G. Pancheri, in: L. Maiani, G. Pancheri, N. Paver (Eds.), The Second DAΦNE Physics Handbook, Vol. II, Frascati, 1995, p. 477; E. Marco, S. Hirenzaki, E. Oset, H. Toki, Phys. Lett. B 470 (1999) 20.
- [3] F.E. Close, Pseudoscalar mesons at DAΦNE, in: L. Maiani, G. Pancheri, N. Paver (Eds.), The DAΦNE Physics Handbook, Vol. II, Frascati, 1992.
- [4] M. Benayoun et al., Phys. Rev. D 59 (1999) 114027.
- [5] J.L. Rosner, Phys. Rev. D 27 (1983) 1101.
- [6] P. Ball, J.-M. Frère, M. Tytgat, Phys. Lett. B 365 (1996) 367.
- [7] A. Bramon, R. Escribano, M.D. Scadron, Eur. Phys. J. C 7 (1999) 271.
- [8] A. Bramon, R. Escribano, M.D. Scadron, Phys. Lett. B 503 (2001) 271.
- [9] T. Feldmann, Int. J. Mod. Phys. A 15 (2000) 159.
- [10] H. Leutwyler, Nucl. Phys. Proc. Suppl. 64 (1998) 223, hep-ph/9709408; R. Kaiser, H. Leutwyler, hep-ph/9806336.
- [11] R. Escribano, J.M. Frere, Phys. Lett. B 459 (1999) 288.
- [12] Th. Feldmann, P. Kroll, B. Stech, Phys. Rev. D 58 (1998).
- [13] F. De Fazio, M.R. Pennington, JHEP 0007 (2000) 051.
- [14] CLEO Collaboration, Phys. Rev. Lett. 85 (2000) 520; BABAR Collaboration, Phys. Rev. Lett. 87 (2001) 221802; BELLE Collaboration, Phys. Lett. B 517 (2001) 309.
- [15] H.Y. Cheng, B. Tseng, Phys. Lett. B 415 (1997) 263; I. Halperin, A. Zhitnitsky, Phys. Rev. D 56 (1997) 7247; A.S. Dighe, M. Gronau, J.L. Rosner, Phys. Rev. Lett. 79 (1997) 4333; A. Ali, J. Chay, C. Greub, P. Ko, Phys. Lett. B 424 (1998) 161; M. Ciuchini, R. Contino, E. Franco, G. Martinelli, L. Silvestrini, Nucl. Phys. B 512 (1998) 3; M.Z. Yang, Y.D. Yang, Nucl. Phys. B 609 (2001) 469; C. Isola, M. Ladisa, G. Nardulli, T.N. Pham, P. Santorelli, Phys. Rev. D 65 (2002) 094005.
- [16] E. Kou, Phys. Rev. D 63 (2001) 054027.
- [17] Particle Data Group, D. Groom et al., Eur. Phys. J. C 15 (2000).
- [18] M.N. Achasov et al., SND Collaboration, JETP Lett. 69 (1999) 97.
- [19] R.R. Akhmetshin et al., CMD-2 Collaboration, Phys. Lett. B 473 (2000) 337; R.R. Akhmetshin et al., CMD-2 Collaboration, Phys. Lett. B 494 (2000) 26.
- [20] KLOE Collaboration, KLOE: a general purpose detector for DAΦNE, LNF-92/019 (IR) 1992; KLOE Collaboration, The KLOE detector. Technical Proposal, LNF-93/002 (IR) 1993.
- [21] S. Guiducci, Status of DAΦNE, in: P. Lucas, S. Webber (Eds.), Proc. of the 2001 Particle Accelerator Conference, Chicago, IL, USA, 2001, pp. 353–355.
- [22] KLOE Collaboration, M. Adinolfi et al., Nucl. Instrum. Methods A 488 (2002) 1.
- [23] KLOE Collaboration, M. Adinolfi et al., Nucl. Instrum. Methods A 482 (2002) 364.
- [24] KLOE Collaboration, M. Adinolfi et al., The KLOE trigger system, to be published in Nucl. Instrum. Methods.
- [25] F. Ambrosino, KLOE note 179, Analysis of  $\phi \rightarrow \eta' \gamma$   $\phi \rightarrow \eta \gamma$  in  $\pi^+ \pi^- \gamma \gamma$  final state, May 2002, <http://www.lnf.infn.it/kloe/pub/knote/kn179.ps>.
- [26] R.R. Akhmetshin et al., Phys. Lett. B 434 (1998) 426.
- [27] G.J. Gounaris, J.J. Sakurai, Phys. Rev. Lett. 21 (1968) 244.